HHS Public Access

Author manuscript

Cancer Lett. Author manuscript; available in PMC 2019 February 28.

Published in final edited form as:

Cancer Lett. 2018 February 28; 415: 198–207. doi:10.1016/j.canlet.2017.11.028.

ELL2 regulates DNA non-homologous end joining (NHEJ) repair in prostate cancer cells

Yachen Zang[1,2], **Laura E. Pascal**[2], **Yibin Zhou**[1,2], **Xiaonan Qiu**[2], **Leizhen Wei**[3,4], **Junkui Ai**[2], **Joel B. Nelson**[2,3], **Mingming Zhong**[2], **Boxin Xue**[1], **Shaoxiong Wang**[1], **Dongrong Yang**[1,*], **Li Lan**[3,4,*], **Yuxi Shan**[1,*], and **Zhou Wang**[2,3,5,*]

[1]Department of Urology, the second Affiliated Hospital of Soochow University, Suzhou, China

[2]Department of Urology, University of Pittsburgh School of Medicine, Pittsburgh, PA 15232, USA

[3]University of Pittsburgh Cancer Institute, University of Pittsburgh School of Medicine, 5117 Centre Avenue, Pittsburgh, PA 15213, USA

[4]Department of Microbiology and Molecular Genetics, University of Pittsburgh School of Medicine, Pittsburgh, PA 15213, USA

[5]Department of Pharmacology and Chemical Biology, University of Pittsburgh School of Medicine, Pittsburgh, PA 15216, USA

Abstract

ELL2 is an androgen-responsive gene that is expressed by prostate epithelial cells and is frequently down-regulated in prostate cancer. Deletion of *Ell2* in the murine prostate induced murine prostatic intraepithelial neoplasia and ELL2 knockdown enhanced proliferation and migration in C4-2 prostate cancer cells. Here, knockdown of ELL2 sensitized prostate cancer cells to DNA damage and overexpression of ELL2 protected prostate cancer cells from DNA damage. Knockdown of ELL2 impaired non-homologous end joining repair but not homologous recombination repair. Transfected ELL2 co-immunoprecipitated with both Ku70 and Ku80 proteins. ELL2 could bind to and co-accumulate with Ku70/Ku80 proteins at sites of DNA damage. Knockdown of ELL2 dramatically inhibited Ku70 and Ku80 recruitment and retention at DNA double-strand break sites in prostate cancer cells. The impaired recruitment of Ku70 and Ku80 proteins to DNA damage sites upon ELL2 knockdown was rescued by re-expression of an ELL2 transgene insensitive to siELL2. This study suggests that ELL2 is required for efficient NHEJ repair via Ku70/Ku80 in prostate cancer cells.

Keywords

ELL2; prostate cancer; DNA damage repair; Non-homologous end joining; Ku70; Ku80

*Corresponding authors.

Conflict of Interest Statement: The authors declare no conflict of interest.

1. Introduction

Prostate cancer is the most common malignancy and the third leading cause of cancer deaths in US males [1]. Elucidating the mechanisms of prostate carcinogenesis may lead to new approaches to prevent and/or treat prostate cancer. Dysregulation of DNA repair mechanisms will facilitate the development and progression of many different types of cancer, including prostate cancer [2; 3; 4]. Non-homologous end joining (NHEJ) and homologous recombination (HR) are two major DNA repair pathways that mediate double strand break (DSB) repair [5]. NHEJ is the most efficient DSB repair pathway and works in all cell cycle phases, whereas HR is a slow multistep process that requires several proteins and operates exclusively during the S and G2 phases of the cell cycle [6; 7]. In NHEJ, the DSB ends are bound by the abundant Ku70/80 heterodimer, which in turn attracts the catalytic subunit DNA-PKcs, that orchestrates the end joining process and phosphorylates itself and other proteins, such as ligase IV and XRCC4, for final rejoining and ligation [8; 9]. It was reported that prostate cancer cells enter into cell cycle arrest (G0) after radiotherapy treatment and therefore rely solely on NHEJ for repair of radiation-induced DSBs [10]. Identification and characterization of factors that can modulate DNA repair mechanisms, especially the NHEJ pathway, in prostate cancer cells will enhance our understanding of the mechanisms of prostate carcinogenesis and may improve the efficacy of radiation therapy of prostate cancer.

ELL2 (elongation factor, RNA polymerase II, 2; previously called eleven-nineteen lysine-rich leukemia 2) is encoded by an androgen-response gene in the prostate [11; 12; 13] and is homologous to ELL and ELL3 [14; 15]. ELL2 suppresses transient pausing of RNA polymerase II activity along the DNA strand and facilitates the transcription process[16]. The ELL family proteins are components of the super elongation complex (SEC) and play a key role in the regulation of HOX gene expression in MLL-based hematological malignancies, by controlling genes involved in early development and in immediate early gene transcription [17; 18]. ELL was recently identified as a component in the little elongation complex (LEC), which is involved in RNA polymerase II transcription of small nuclear RNA (snRNA) genes [19]. ELL1 is frequently translocated with the MLL gene on chromosome 11q23 in acute myeloid leukemia [20]. ELL1 and ELL2 interact with ELL-associated factors 1 and 2 (EAF1 and EAF2) resulting in enhanced ELL elongation activity [21; 22]. ELL2 has been identified as an androgen response gene in immortalized normal human prostate epithelial cells [12] as well as prostate cancer cell lines LNCaP [11; 23] and C4-2 [24]. Conditional deletion of *Ell2* in the murine prostate induced increased epithelial proliferation, increased microvessel density and murine prostatic intraepithelial neoplasia [24]. Knockdown of ELL2 in combination with retinoblastoma (RB) enhanced prostate cancer cell proliferation, migration and invasion [13]. ELL2 expression was down-regulated in high Gleason score prostate cancer specimens [13]. In large-scale genomic datasets, ELL2 and ELL2 target genes were upregulated in prostate cancers with a neuroendocrine phenotype, while down-regulation of ELL2 and its target genes was associated with prostate adenocarcinoma [24]. Cumulatively, these studies suggest that ELL2 may play a significant role in maintaining prostate homeostasis.

We have recently reported that EAF2, an ELL2 binding partner, can enhance DNA repair through Ku70/Ku80 recruitment in the prostate [25]. This led to our hypothesis that ELL2 can regulate DNA repair through Ku70/Ku80 in prostate cancer cells. In the current study, we have investigated the function of ELL2 in DNA repair, particularly in the recruitment and retention of NHEJ pathway proteins Ku70/Ku80 to damaged DNA.

2. Material and Methods

2.1. Cell Culture, Overexpression, and Knockdown

LNCaP, PC3 and HEK293 cells were obtained from American Type Culture Collection (Manassas, VA), and C4-2 cells were obtained as a kind gift from Leland K. Chung (Cedars-Sinai Medical Center). LNCaP, PC3 and C4-2 were maintained in RPMI-1640 medium (10-040-CV, Corning cellgro, Corning Inc., Corning, NY) supplemented with 10% fetal bovine serum (FBS) (S11150, Atlanta Biologicals, Flowery Branch, GA), 1% glutamine, 100 U/ml penicillin, and 100 μg/ml streptomycin (Invitrogen, Carlsbad, CA). HEK293 cells were maintained in DMEM medium (12-604F, Lonza, Basel, Switzerland) supplemented with 10% FBS, 1% glutamine, 100 U/ml penicillin, and 100 μg/ml streptomycin (Invitrogen). Cell lines LNCaP and C4-2 were authenticated in 2016 using DNA fingerprinting by examining microsatellite loci in a multiplex PCR reaction (AmpFlSTR® Identifiler® PCR Amplification Kit, Applied Biosystems, Foster City, CA) by the University of Pittsburgh Cell Culture and Cytogenetics Facility. PC3 and HEK293 cell lines were obtained from ATCC in 2016. ATCC performed authentication for HEK293 and cell lines using short tandem repeat profiling.

H1299 dA3-1#1, a subline of human lung cancer cells obtained by transfecting a plasmid DNA containing two I-SceI sites into H1299 cells was used as model of assay for NHEJ of chromosomal DSBs. HeLa pDR-GFP cells containing a recombination substrate DR-GFP in HeLa cells was used as a model of assay for HR frequency of chromosomal DNA. H1299 dA3-1#1 and HeLa pDR-GFP cells were cultured in RPMI-1640 medium. No authentication was performed for H1299 dA3-1#1, H1299 dA3-1#1 or HeLa pDR-GFP cells.

pCHV-3NLS-I-SceI, Flag-tagged ELL2, GFP and RFP-tagged human Ku70, Ku80 expression vectors were described previously [25]. GFP-tagged human ELL2 expression vectors were constructed by PCR cloning. For overexpression experiments, cells were transiently transfected with indicated expression vector(s) using PolyJet In Vitro Transfection reagent (SL100688, SignaGen Laboratories, Rockville, MD) according to the manufacturer's instructions. For knockdown experiments, cells were transfected with control siRNA (sc-37007 Santa Cruz Biotechnology, Dallas, TX) or siRNAs targeting ELL2 using DharmaFECT siRNA transfection reagent (T-2001-03, Dharmacon, Lafayette, CO). All siRNA sequences against ELL2 are ordered from IDT (Coralville, IA) and listed in Table 1. siELL2-1 and siELL2-2 were used to confirm that the impact of siRNAs was due to knockdown of specific gene(s) and not because of their potential off-target effects. siELL2-3 could knockdown endogenous ELL2, but cannot affect transfected ELL2, so this siRNA sequence was used in the experiment of re-expression of ELL2 after ELL2 was depleted.

2.2. Western Blot Analysis

At the completion of each experiment, cells were lysed in modified radioimmune precipitation assay buffer [50 mm Tris (pH 7.4), 1% Igepal CA-630, 0.25% Na-deoxycholate, 150 mm NaCl, 1 mm EDTA (pH 8.0), 1 mm NaF, 2 mm phenylmethylsulfonylfluoride, 1 mm Na_3VO_4, and protease inhibitor cocktail (Sigma-Aldrich, St. Louis, MO)]. The cell lysates were then prepared and resolved on sodium dodecyl sulfate (SDS) polyacrylamide gel electrophoresis, and proteins were transferred to polyvinylidene difluoride membranes. The membranes were incubated overnight at 4°C with antibodies. Following secondary antibody incubation, immunoreactive proteins were visualized with an enhanced chemiluminescence detection system (Bio-Rad Laboratories, Hercules, CA). Antibodies used are listed in Supplemental Table 1.

2.3. Colony formation assay

C4-2 cells were treated with siELL2 or control siRNA for 48 hours, then treated with doxorubicin for an additional 24 hours. The culture medium was replaced, and cells were plated in 10-cm culture plates at a density of 2000 cells/plate, and incubated for 14 days and then fixed with 10% methanol, stained with 0.05% crystal violet, and colonies were counted by Image-Pro Plus software (Media Cybernetics, Inc., Rockville, MD). The average normalized surviving fractions from three independent experiments were calculated.

2.4. Comet Assay

C4-2 cells were treated with siRNA for 48 hours, then treated with γ-irradiation or doxorubicin and collected for DNA damage analysis. C4-2 cells were treated with siELL2 or control siRNA 48 hours. Then the cells were treated with 0, 1, or 4 Gy γ radiation and collected for DNA damage analysis 6 hours after irradiation, or the cells were treated with various concentrations of doxorubicin (Sigma-Aldrich) for an additional 24 hours. DNA damage was quantified by using a neutral comet assay (Comet Assay Kit, Trevigen, Gaithersburg, MD) according to the instruction of the kit. In brief, the cells were washed with 1 × PBS and trypsinized to resuspend into 5×10^5/ml cell solution in 1 × PBS. Then cells were combined with molten LMAgarose at 37°C and immediately pipetted onto a slide. Slides were immersed in lysis solution for electrophoresis and immersed in DNA precipitation solution, then slides were stained with SYBR Green I. Average tail moments from 50 cells per sample were obtained using Comet Assay IV software (Perceptive Instruments, Bury St. Edmunds, UK), and data are shown as mean values with standard errors from three or more independent experiments.

2.5. NHEJ and HR Assay

H1299 dA3-1#1, a subline of human lung cancer cells obtained by transfecting a plasmid DNA containing two I-SceI sites into H1299 cells was used as model of assay for NHEJ of chromosomal DSBs. HeLa pDRGFP cells containing a recombination substrate DR-GFP in HeLa cells was used as a model of assay for HR frequency of chromosomal DNA. pCMV-NLS-I-SceI to express I-SceI was introduced by transfection with PolyJet reagent into H1299 dA3-1#1 cells (for NHEJ) or HeLa pDRGFP cells (for HR) pretransfected with siRNA for 48 hours using DharmaFECT reagent. For FACS analysis, cells were harvested

by trypsinization, washed with PBS, and applied to the FACSCalibur Flow Cytometer (BD Biosciences, San Jose, CA). EGFP-positive cells were counted using BD Cellquest Pro software (BD Biosciences).

2.6. Immunoprecipitation

For co-immunoprecipitation, HEK293 cells in 10-cm culture plates were transiently transfected with 6 μg of the indicated plasmids, cultured for 48 hours after transfection, and lysed in lysis buffer (150 mM NaCl, 20 mM Tris-HCl, 1.5 mM $MgCl_2$, 1% NP-40, 15% glycerol, 2 mM EDTA) with protease inhibitor cocktails (P8345-5ML, Sigma-Aldrich) at a dilution of 1:100. After precleaning cell lysates with protein A/G plus-agarose beads (sc-2003, Santa Cruz) for 1 hour and blocking anti-Flag (A2220-1ML, Sigma-Aldrich)/anti-GFP antibody-conjugated agarose beads with 2.5% albumin/bovine (94349-60-7, Acros Organics, Thermo Fisher, Waltham, MA) for 1 hour, cell lysates were added to anti-FLAG/anti-GFP antibody-conjugated agarose beads and rotated at 4° C for 1.5 hours. The beads were washed using lysis buffer four times. Immunoprecipitates and total cell lysates were boiled in SDS loading buffer for 10 minutes and then subjected to Western blot analysis using anti-Flag antibody or anti-GFP antibody.

2.7. Laser Micro-irradiation

For laser irradiation, C4-2 cells were cultured in 35 mm bottom dishes (P35GCOL-0-10-C, MatTek Corporation, Ashland, MA) and transiently transfected with 1 μg of the indicated plasmids, cultured for 48 hours after transfection. Then cells treated with 100 μM 8-methoxypsoralen (8-MOP) for 5 minutes prior to laser micro-irradiation. Fluorescence images were obtained and processed using an FV-500 confocal scanning laser microscopy system (Olympus, Tokyo, Japan). The power of the 405 nm laser (500 scans with 1.6 μW/scan) was adjusted with time at a final output of 800 μW after passing through the lens. Cells were incubated with in glass-bottomed dishes, which were covered with microscopy live-cell imaging chambers (Olympus) to prevent evaporation on the 37°C heating plate. At least ten cells were irradiated in every experiment, and representative data are shown. For evaluation of accumulation and kinetics, the mean intensity of each accumulated line was obtained after subtraction of the background intensity in the irradiated cells, and mean values were obtained from at least three independent cells.

3. Results

3.1. ELL2 protects prostate cancer cells from doxorubicin- or γ-irradiation-induced DNA damage

Previously, we showed that ELL2 binding partners, EAF1 and EAF2, could play a role in DNA repair in prostate cancer cells [25]. Here, we tested the role of ELL2 in DNA repair in prostate cancer cell lines LNCaP, C4-2 and PC3 cells. Cells were treated with siRNA knockdown of ELL2 followed by the induction of DSB DNA damage by doxorubicin hydrochloride (Dx) or γ-irradiation. Both Dx and γ-irradiation induce DNA damage mainly in the form of DSBs [26]. DNA damage marker phospho-Histone H2ax (γH2AX) levels, a marker of DNA damage [27; 28], was elevated in response to Dx or γ-irradiation treatment in these cell lines (Figure 1). We previously showed that γH2AX levels gradually increased

over time in response to 0.5 μg/ml Dx to a peak level at 24-36 hours post-induction in LNCaP cells and by 60 hours γH2AX levels were not detected in control cells, whereas cells over-expression EAF1 recovered within 48 hours [25]. Increased γH2AX was detected at 5 hours post-exposure in LNCaP cells treated with γ-irradiation and at 24 hours post-exposure in mice [25]. Additionally, increased γH2AX levels were detectable in MCF-7 breast cancer cells following γ-irradiation [29]. Therefore, we examined γH2AX levels in cells treated with Dx at 24 hours post-exposure and at 6 hours post-exposure for cells treated with γ-irradiation. Similar results were achieved in C4-2 cells treated with a second set of siRNA to control for potential off-target effects of siRNA (Supplemental Figure S1). The enhanced γH2AX levels in p53-negative PC3 cells with ELL2 knockdown upon Dx or γ-irradiation treatment (Figure 1C, E) suggested that p53 was not necessary for ELL2 modulation of DNA repair.

Knockdown of ELL2 in C4-2 cells also resulted in longer comet tails compared with control group in neutral comet assay (Figure 2A, B). Since downregulation of ELL2 sensitized cells to DNA damage, we examined the effects of overexpression of ELL2 on C4-2 cells exposed to DNA damage. When compared to C4-2/Flag using γH2ax as a marker of DNA damage, C4-2/Flag-ELL2 cells were less sensitive to Dx- or γ-irradiation-induced DNA damage (Figure 2C, D). These results suggest that ELL2 can enhance the repair of DNA damage induced by DSBs.

3.2 ELL2 silencing reduces C4-2 cell colony formation upon Dx treatment

The effect of ELL2 silencing on colony numbers in C4-2 cells is presented in Figure 3. As knockdown of ELL2 could enhance prostate cancer cell proliferation, cell clone numbers were significantly increased when ELL2 was knockdown without Dx treatment. When the cells were treated with Dx (0.2 μg/ml), knockdown of ELL2 reduced colony formation significantly. These results suggested that DNA damage caused by Dx in prostate cancer cells could be recovered by more efficient DNA damage repair in the presence of ELL2, whereas in the absence of ELL2, more cells died due to unrepaired DNA damage, and colony formation was reduced.

3.3. Knockdown of ELL2 impairs non-homologous end joining (NHEJ) repair

Given NHEJ and HR are the major pathways to repair DSBs in cells [3; 5; 30], we utilized the previously established H1299dA3-1#1 and Hela pDR-GFP cell models [31; 32] to test the role of ELL2 in these two repair pathways (Figure 4). Briefly, H1299 dA3-1#1 cells carry a stably integrated DNA fragment with two recognition sites for the I-SceI endonuclease (Figure 4A). Transiently expressed I-SceI protein cleaves the I-SceI sites (arrowheads) and produces DSBs with incompatible ends in the substrate. NHEJ repair of two broken DNA ends of chromosomal DNA results in EGFP expression of the EGFP gene driven by an upstream CMV promoter, which provides a quantitative measurement of DNA repair events. Knockdown of ELL2 reduced the percentage of GFP-positive cells compared with cells treated with siRNA control (Figure 4A), indicating that ELL2 was required for efficient NHEJ.

The Hela pDR-GFP-based assay for HR repair [31; 32] measures HR frequency of chromosomal DNA containing a recombination substrate DR-GFP in HeLa cells. Briefly, a gene conversion event within two differentially mutated GFP genes, a GFP gene harboring a single I-SceI site (arrowhead) with in-frame stop codons, SceGFP, and a downstream internal GFP fragment (iGFP), results in the expression of intact GFP protein (Figure 4B). No significant difference was detected in the percentage of GFP-positive cells between siELL2-treated and siRNA control groups (Figure 4B), suggesting that ELL2 did not affect the HR repair pathway.

3.4. ELL2 protein co-accumulates with and binds to Ku70/Ku80 proteins at the DNA damage sites

The core NHEJ proteins consist of DNA-dependent protein kinase (DNA-PK) and the ligase IV/XRCC4/XLF complex [33; 34]. Formation of the Ku70/80 heterodimer, which is the DNA binding component of DNA-PK, is an initiating event of NHEJ [34]. Since ELL2 could modulate NHEJ repair of DSBs, we tested if ELL2 could co-accumulate with Ku70 and Ku80 proteins at DSBs induced by laser microirradiation in C4-2 cells. GFP-ELL2 protein accumulated at sites of DNA damage induced by 405 nm laser microirradiation (Figure 5). Co-transfection of GFP-ELL2 and RFP-Ku70 or RFP-Ku80 in C4-2 cells subjected to laser microirradiation showed that GFP-ELL2 co-accumulated at DSB sites with RFP-Ku70 or RFP-Ku80 (Figure 5). All three proteins responded to microirradiation within seconds, which prevented us from distinguishing the order of their accumulation at DSBs.

Co-localization of proteins suggests the potential for their physical interaction. HEK293 cells were transiently transfected with Flag-ELL2 plus GFP, GFP-Ku70, or GFP-K80 expression vector. GFP-Ku70 and Ku80 were co-precipitated with Flag-ELL2 both in the absence and presence of Dx when anti-GFP antibody-conjugated agarose beads were used (Figure 6). This suggested that ELL2 physically interacted with Ku70 or Ku80, and that they could be present in the same protein complex. In addition, GFP-Ku80 was expressed at a lower level that GFP-Ku70 in transfected cells, yet GFP-Ku80 pulled down more Flag-ELL2 than GFP-Ku70, suggesting ELL2 and Ku80 may bind together more tightly than ELL2 and Ku70. This finding is consistent with the observation that Flag-ELL2 immunoprecipitation pulled down GFP-Ku80 but not GFP-Ku70 (Supplemental Figure S2).

3.5. Knockdown of ELL2 impairs recruitment of Ku70/Ku80 at sites of DSBs

The first step of NHEJ repair of DSBs is Ku70/80 heterodimer binding to the DNA ends, and recruitment of Ku70 and Ku80 heterodimers to DSBs is a key step to initiate NHEJ[34]. As it was demonstrated that knockdown of ELL2 impaired NHEJ repair of DSBs (see Figure 4A), we wanted to determine the effect of ELL2 knockdown on Ku70 and Ku80 recruitment in response to laser microirradiation. Knockdown of ELL2 inhibited Ku70 and Ku80 accumulation and retention at DSB sites dramatically in C4-2 cells (Figure 7A and 7B). As a control, it was shown that knockdown of ELL2 did not affect the levels of Ku70 and Ku80 proteins (Supplemental Figure S3). Since knockdown of ELL2 impairs the recruitment of Ku70 and Ku80 at laser microirradiation DSBs sites, we examined the effect of re-expression of ELL2 on Ku70 and Ku80 recruitment. The impaired recruitment of Ku

proteins to DNA damage sites upon ELL2 knockdown using another siRNA was rescued by re-expression of an ELL2 transgene insensitive to siELL2 in C4-2 cells (Figure 7C and 7D), suggesting that siELL2 inhibition of the Ku proteins recruitment was indeed mediated through ELL2 knockdown. Taken together, these data strongly suggest that ELL2 works together with Ku proteins in the induction of DNA repair.

4. Discussion

This study presents evidence for ELL2 as a key regulator of DNA repair in prostate cancer cells. Knockdown of ELL2 sensitized prostate cancer cells to DNA damage and overexpression of ELL2 protected prostate cancer cells from DNA damage. Interestingly, ELL2 expression levels increased in response to DNA damage in some experiments (for example Figure 1A and Figure 2C). This increased expression was not always reproducible and could be due to variations in growth conditions. Future studies will be required to determine the mechanism behind the increase in ELL2 in response to DNA damage. Knockdown of ELL2 impaired NHEJ repair, but not HR. Transfected ELL2 co-immunoprecipitated with both Ku70 and Ku80 proteins. ELL2 could bind to and co-accumulate with Ku70/Ku80 proteins at sites of DNA damage. Knockdown of ELL2 dramatically inhibited Ku70 and Ku80 recruitment and retention at DSB sites in prostate cancer cells. These findings suggest that ELL2 is required for efficient NHEJ repair of damaged DNA via Ku70/Ku80, providing mechanistic insights into DNA repair and prostate carcinogenesis.

Our study confirmed that Ku70 and Ku80 proteins accumulate rapidly at the DSBs sites after laser micro-irradiation, and ELL2 co-accumulates rapidly at the same DSBs sites, suggesting that ELL2 enhances NHEJ repair the recruitment of Ku70 and Ku80 to DSBs sites. This was further supported by the inhibition of Ku70/Ku80 recruitment to DNA damage sites upon ELL2 knockdown. The impaired recruitment of Ku proteins at the DSB site upon ELL2 knockdown was rescued by re-expression of siRNA-resistant ELL2. These observations suggested that ELL2 is required for efficient NHEJ repair and that ELL2 down-regulation in prostate cancer could promote genomic DNA mutations and/or deletions, which are key steps in carcinogenesis.

The enhanced recruitment of Ku70/80 to DNA damage sites by ELL2 is likely mediated through physical interactions between ELL2 and Ku70/80 proteins. This possibility is supported by co-IP of ELL2 and Ku70/80. In addition, knockdown or overexpression of ELL2 did not change the expression levels of Ku70 and Ku80 proteins, suggesting that reduced Ku proteins recruitment and retention at DSBs upon ELL2 knockdown was not due to reduced Ku protein expression. Since ELL2 co-precipitation with Ku80 appeared much more efficient than Ku70 in our experiments, ELL2 interaction Ku70/80 complexes may be predominantly mediated through Ku80. It is still not clear if ELL2 binds to Ku70/80 directly or mediated through other factors. Further studies, will be needed to address how ELL2 interacts with Ku70/80 and enhances their recruitment at DNA damage sites.

ELL2 and EAF2 can functionally interact and recent findings suggest that ELL2 may also act as a tumor suppressor in the prostate [13]. Recently, we showed that EAF2 and its

homolog EAF1 were key regulators of DNA damage repair through the NHEJ pathway in the prostate [25]. The findings that both ELL2 and EAF2 can regulate NHEJ repair via Ku70/80 suggest that ELL and EAF family proteins can act on the same signaling pathways, which is consistent with a model that ELL and EAF family proteins work together and are present in the same protein complex. Ai et al., reported that EAF1 and EAF2 were non-redundant in their regulation of Ku70/Ku80 recruitment and that knockdown of EAF1 or EAF2 sensitized prostate cancer cells to DNA damage [25]. Future studies of the impact of ELL2 knockdown in the presence or absence of EAF2 and/or EAF1 will be important in further elucidating the role of the ELL and EAF family proteins in DNA damage repair. Given that ELL2 and EAF2 are both important in DNA repair, prostate tumors with ELL2 and/or EAF2 down-regulation may be more sensitive to radiation therapy.

In summary, our studies revealed that ELL2 protein is a key regulator of Ku70/Ku80-mediated DNA double-strand break repair via NHEJ. An important mechanism for ELL2 loss to induce prostate carcinogenesis may involve impaired DNA damage response and repair. Future studies will be required to determine the mechanism of ELL2 stimulation of Ku proteins recruitment in DNA damage response in prostate cancer cells and to test if ELL2 could also modulate other DNA repair proteins, in addition to Ku70/80.

Supplementary Material

Refer to Web version on PubMed Central for supplementary material.

Acknowledgments

This work was funded in part by grants 9R01CA186780, 1P50CA180995, 1R50CA211242, and T32 DK007774 as well as by the Tippins Foundation (LEP), and the Mellam Family Foundation (LEP). This project used the UPMC Hillman Cancer Center Animal Facility and the Tissue and Research Pathology Services (TARPS) and was supported in part by award P30CA047904.

References

1. Siegel RL, Miller KD, Jemal A. Cancer statistics, 2016 CA: a cancer journal for clinicians. 2016; 66:7–30. [PubMed: 26742998]
2. Jaamaa S, Af Hallstrom TM, Sankila A, Rantanen V, Koistinen H, Stenman UH, Zhang Z, Yang Z, De Marzo AM, Taari K, Ruutu M, Andersson LC, Laiho M. DNA damage recognition via activated ATM and p53 pathway in nonproliferating human prostate tissue. Cancer research. 2010; 70:8630–8641. [PubMed: 20978201]
3. Zhang Z, Yang Z, Jaamaa S, Liu H, Pellakuru LG, Iwata T, af Hallstrom TM, De Marzo AM, Laiho M. Differential epithelium DNA damage response to ATM and DNA-PK pathway inhibition in human prostate tissue culture. Cell cycle. 2011; 10:3545–3553. [PubMed: 22030624]
4. Kurfurstova D, Bartkova J, Vrtel R, Mickova A, Burdova A, Majera D, Mistrik M, Kral M, Santer FR, Bouchal J, Bartek J. DNA damage signalling barrier, oxidative stress and treatment-relevant DNA repair factor alterations during progression of human prostate cancer. Molecular oncology. 2016; 10:879–894. [PubMed: 26987799]
5. Jackson SP, Bartek J. The DNA-damage response in human biology and disease. Nature. 2009; 461:1071–1078. [PubMed: 19847258]
6. Haines JW, Coster M, Bouffler SD. Impairment of the non-homologous end joining and homologous recombination pathways of DNA double strand break repair: Impact on spontaneous and radiation-induced mammary and intestinal tumour risk in Apc min/+ mice. DNA repair. 2015; 35:19–26. [PubMed: 26435054]

7. Takata M, Sasaki MS, Sonoda E, Morrison C, Hashimoto M, Utsumi H, Yamaguchi-Iwai Y, Shinohara A, Takeda S. Homologous recombination and non-homologous end-joining pathways of DNA double-strand break repair have overlapping roles in the maintenance of chromosomal integrity in vertebrate cells. The EMBO journal. 1998; 17:5497–5508. [PubMed: 9736627]
8. Jeggo PA. Identification of genes involved in repair of DNA double-strand breaks in mammalian cells. Radiation research. 1998; 150:S80–91. [PubMed: 9806611]
9. Ahnesorg P, Smith P, Jackson SP. XLF interacts with the XRCC4-DNA ligase IV complex to promote DNA nonhomologous end-joining. Cell. 2006; 124:301–313. [PubMed: 16439205]
10. Tarish FL, Schultz N, Tanoglidi A, Hamberg H, Letocha H, Karaszi K, Hamdy FC, Granfors T, Helleday T. Castration radiosensitizes prostate cancer tissue by impairing DNA double-strand break repair. Science translational medicine. 2015; 7:312re311.
11. Nelson PS, Clegg N, Arnold H, Ferguson C, Bonham M, White J, Hood L, Lin B. The program of androgen-responsive genes in neoplastic prostate epithelium. Proceedings of the National Academy of Sciences of the United States of America. 2002; 99:11890–11895. [PubMed: 12185249]
12. Bolton EC, So AY, Chaivorapol C, Haqq CM, Li H, Yamamoto KR. Cell- and gene-specific regulation of primary target genes by the androgen receptor. Genes & development. 2007; 21:2005–2017. [PubMed: 17699749]
13. Qiu X, Pascal LE, Song Q, Zang Y, Ai J, O'Malley KJ, Nelson JB, Wang Z. Physical and Functional Interactions between ELL2 and RB in the Suppression of Prostate Cancer Cell Proliferation, Migration, and Invasion. Neoplasia. 2017; 19:207–215. [PubMed: 28167296]
14. Shilatifard A, Duan DR, Haque D, Florence C, Schubach WH, Conaway JW, Conaway RC. ELL2, a new member of an ELL family of RNA polymerase II elongation factors. Proceedings of the National Academy of Sciences of the United States of America. 1997; 94:3639–3643. [PubMed: 9108030]
15. Miller T, Williams K, Johnstone RW, Shilatifard A. Identification, cloning, expression, and biochemical characterization of the testis-specific RNA polymerase II elongation factor ELL3. The Journal of biological chemistry. 2000; 275:32052–32056. [PubMed: 10882741]
16. Martincic K, Alkan SA, Cheatle A, Borghesi L, Milcarek C. Transcription elongation factor ELL2 directs immunoglobulin secretion in plasma cells by stimulating altered RNA processing. Nature immunology. 2009; 10:1102–1109. [PubMed: 19749764]
17. Liu M, Hsu J, Chan C, Li Z, Zhou Q. The ubiquitin ligase Siah1 controls ELL2 stability and formation of super elongation complexes to modulate gene transcription. Molecular cell. 2012; 46:325–334. [PubMed: 22483617]
18. Lin C, Garrett AS, De Kumar B, Smith ER, Gogol M, Seidel C, Krumlauf R, Shilatifard A. Dynamic transcriptional events in embryonic stem cells mediated by the super elongation complex (SEC). Genes & development. 2011; 25:1486–1498. [PubMed: 21764852]
19. Smith ER, Lin C, Garrett AS, Thornton J, Mohaghegh N, Hu D, Jackson J, Saraf A, Swanson SK, Seidel C, Florens L, Washburn MP, Eissenberg JC, Shilatifard A. The little elongation complex regulates small nuclear RNA transcription. Molecular cell. 2011; 44:954–965. [PubMed: 22195968]
20. Yu X, Ai J, Cai L, Jing Y, Wang D, Dong J, Pascal LE, Zhang J, Luo R, Wang Z. Regulation of tumor suppressor EAF2 polyubiquitination by ELL1 and SIAH2 in prostate cancer cells. Oncotarget. 2016; 7:29245–29254. [PubMed: 27058417]
21. Simone F, Luo RT, Polak PE, Kaberlein JJ, Thirman MJ. ELL-associated factor 2 (EAF2), a functional homolog of EAF1 with alternative ELL binding properties. Blood. 2003; 101:2355–2362. [PubMed: 12446457]
22. Kong SE, Banks CA, Shilatifard A, Conaway JW, Conaway RC. ELL-associated factors 1 and 2 are positive regulators of RNA polymerase II elongation factor ELL. Proceedings of the National Academy of Sciences of the United States of America. 2005; 102:10094–10098. [PubMed: 16006523]
23. Hieronymus H, Lamb J, Ross KN, Peng XP, Clement C, Rodina A, Nieto M, Du J, Stegmaier K, Raj SM, Maloney KN, Clardy J, Hahn WC, Chiosis G, Golub TR. Gene expression signature-

based chemical genomic prediction identifies a novel class of HSP90 pathway modulators. Cancer cell. 2006; 10:321–330. [PubMed: 17010675]

24. Pascal LE, Masoodi KZ, Liu J, Qiu X, Song Q, Wang Y, Zang Y, Yang T, Rigatti LH, Chandran U, Colli LM, Vencio RZN, Lu Y, Zhang J, Wang Z. Conditional deletion of ELL2 induces murine prostate intraepithelial neoplasia. J Endocrinol. 2017; 235:123–136. [PubMed: 28870994]
25. Ai J, Pascal LE, Wei L, Zang Y, Zhou Y, Yu X, Gong Y, Nakajima S, Nelson JB, Levine AS, Lan L, Wang Z. EAF2 regulates DNA repair through Ku70/Ku80 in the prostate. Oncogene. 2017; 36:2054–2065. [PubMed: 27721405]
26. Jackson SP. Sensing and repairing DNA double-strand breaks. Carcinogenesis. 2002; 23:687–696. [PubMed: 12016139]
27. Kuo LJ, Yang LX. Gamma-H2AX - a novel biomarker for DNA double-strand breaks. In vivo. 2008; 22:305–309. [PubMed: 18610740]
28. Mah LJ, El-Osta A, Karagiannis TC. gammaH2AX: a sensitive molecular marker of DNA damage and repair. Leukemia. 2010; 24:679–686. [PubMed: 20130602]
29. Chiba N, Comaills V, Shiotani B, Takahashi F, Shimada T, Tajima K, Winokur D, Hayashida T, Willers H, Brachtel E, Vivanco MD, Haber DA, Zou L, Maheswaran S. Homeobox B9 induces epithelial-to-mesenchymal transition-associated radioresistance by accelerating DNA damage responses. Proceedings of the National Academy of Sciences of the United States of America. 2012; 109:2760–2765. [PubMed: 21930940]
30. Ciccia A, Elledge SJ. The DNA damage response: making it safe to play with knives. Molecular cell. 2010; 40:179–204. [PubMed: 20965415]
31. Ogiwara H, Ui A, Otsuka A, Satoh H, Yokomi I, Nakajima S, Yasui A, Yokota J, Kohno T. Histone acetylation by CBP and p300 at double-strand break sites facilitates SWI/SNF chromatin remodeling and the recruitment of non-homologous end joining factors. Oncogene. 2011; 30:2135–2146. [PubMed: 21217779]
32. Lan L, Ui A, Nakajima S, Hatakeyama K, Hoshi M, Watanabe R, Janicki SM, Ogiwara H, Kohno T, Kanno S, Yasui A. The ACF1 complex is required for DNA double-strand break repair in human cells. Molecular cell. 2010; 40:976–987. [PubMed: 21172662]
33. Burma S, Chen BP, Chen DJ. Role of non-homologous end joining (NHEJ) in maintaining genomic integrity. DNA repair. 2006; 5:1042–1048. [PubMed: 16822724]
34. Lieber MR. The mechanism of human nonhomologous DNA end joining. The Journal of biological chemistry. 2008; 283:1–5. [PubMed: 17999957]

Abbreviations

DNA	deoxyribonucleic acid
DNA-PK	DNA-dependent protein kinase
DNA-PKcs	DNA-dependent protein kinase, catalytic subunit
DSB	double strand break
Dx	doxorubicin hydrocholoride
EAF1	ELL-associated factor 1
EAF2	ELL-associated factor 2
ELL	elongation factor, RNA polymerase II
ELL2	elongation factor, RNA polymerase II, 2
ELL3	elongation factor, RNA polymerase II, 3

FACS	fluorescence activated cell sorting
GFP	green fluorescent protein
γH2AX	phospho-Histone H2ax
HOX	homeobox protein Hox-A3a-like
HR	homologous recombination
iGFP	internal green fluorescent protein fragment
LEC	little elongation complex
MLL	lysine methyltransferase 2A
NHEJ	non-homologous end joining
PCR	polymerase chain reaction
RB	retinoblastoma
RFP	red fluorescent protein
RNA	ribonucleic acid
snRNA	small nuclear
SEC	super elongation complex
XRCC4	x-ray repair cross complementing 4

Highlights

- ELL2 knockdown sensitized prostate cancer cells to DNA damage, while overexpression of ELL2 protected prostate cancer cells from DNA damage.
- ELL2 knockdown impaired non-homologous end joining repair but not homologous recombination repair.
- Transfected ELL2 co-immunoprecipitated with both Ku70 and Ku80 proteins; and ELL2 could bind to and co-accumulate with Ku70/Ku80 proteins at sites of DNA damage.
- Knockdown of ELL2 dramatically inhibited Ku70 and Ku80 recruitment and retention at DNA double-strand break sites in prostate cancer cells, while re-expression of ELL2 rescued the recruitment of Ku70 and Ku80 proteins to DNA damage sites.
- ELL2 is required for efficient NHEJ repair via Ku70/Ku80 in prostate cancer cells.

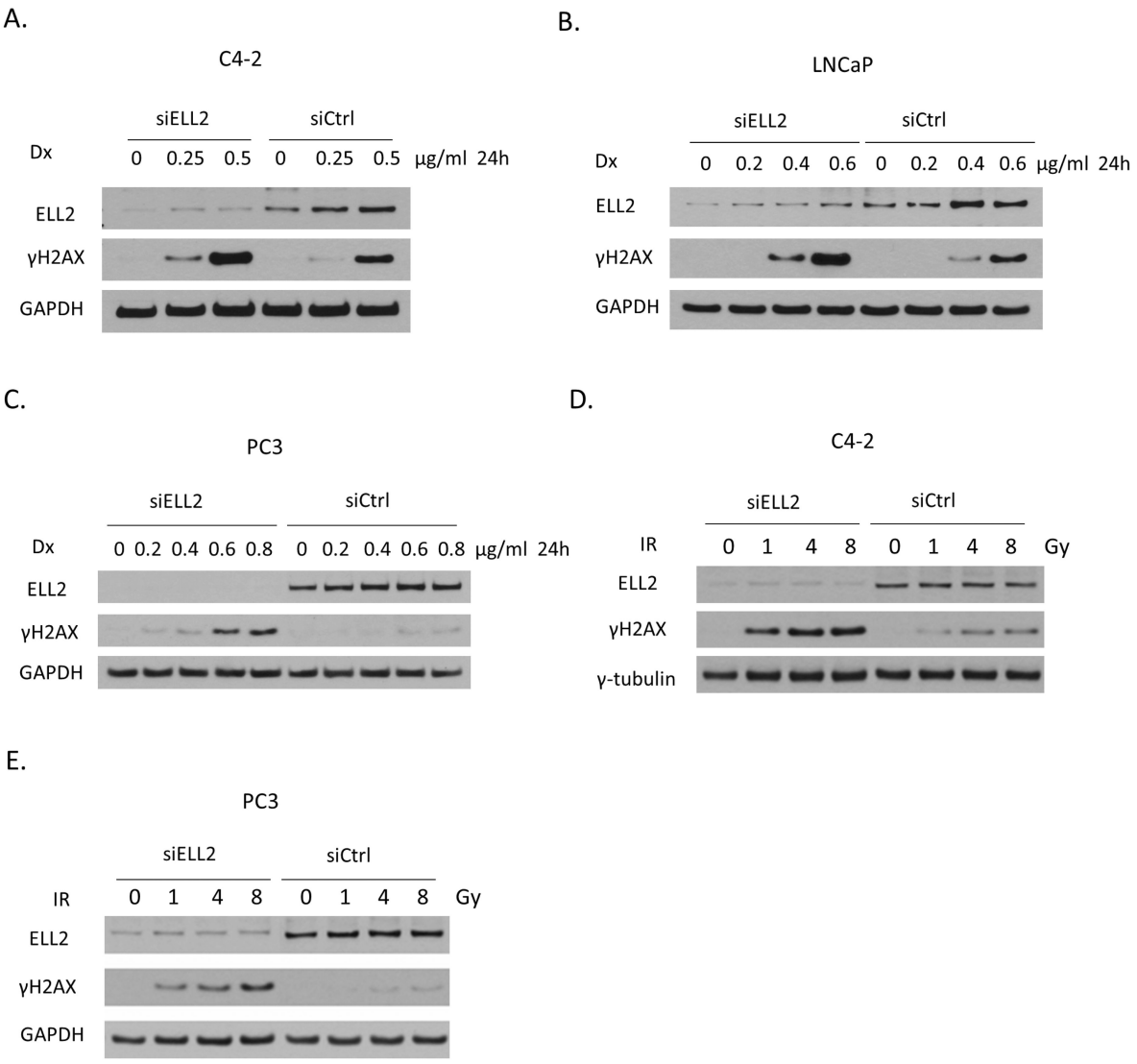

Figure 1. ELL2 protects prostate cancer cells from doxorubicin- or γ-irradiation-induced DNA damage

Expression of γH2AX in (A) C4-2, (B) LNCaP, and (C) PC3 cells treated with siRNA targeting ELL2 (siELL2) or control siRNA (siCtrl) for 48 hours and then treated with indicated concentrations of doxorubicin (Dx, μg/ml) for additional 24 hours. Effect of siELL2 on γH2AX induction by γ-irradiation in (D) C4-2 and (E) PC3 cells. Cells were irradiated at indicated dosages 48 hours after ELL2 knockdown and collected 6 hours after the irradiation.

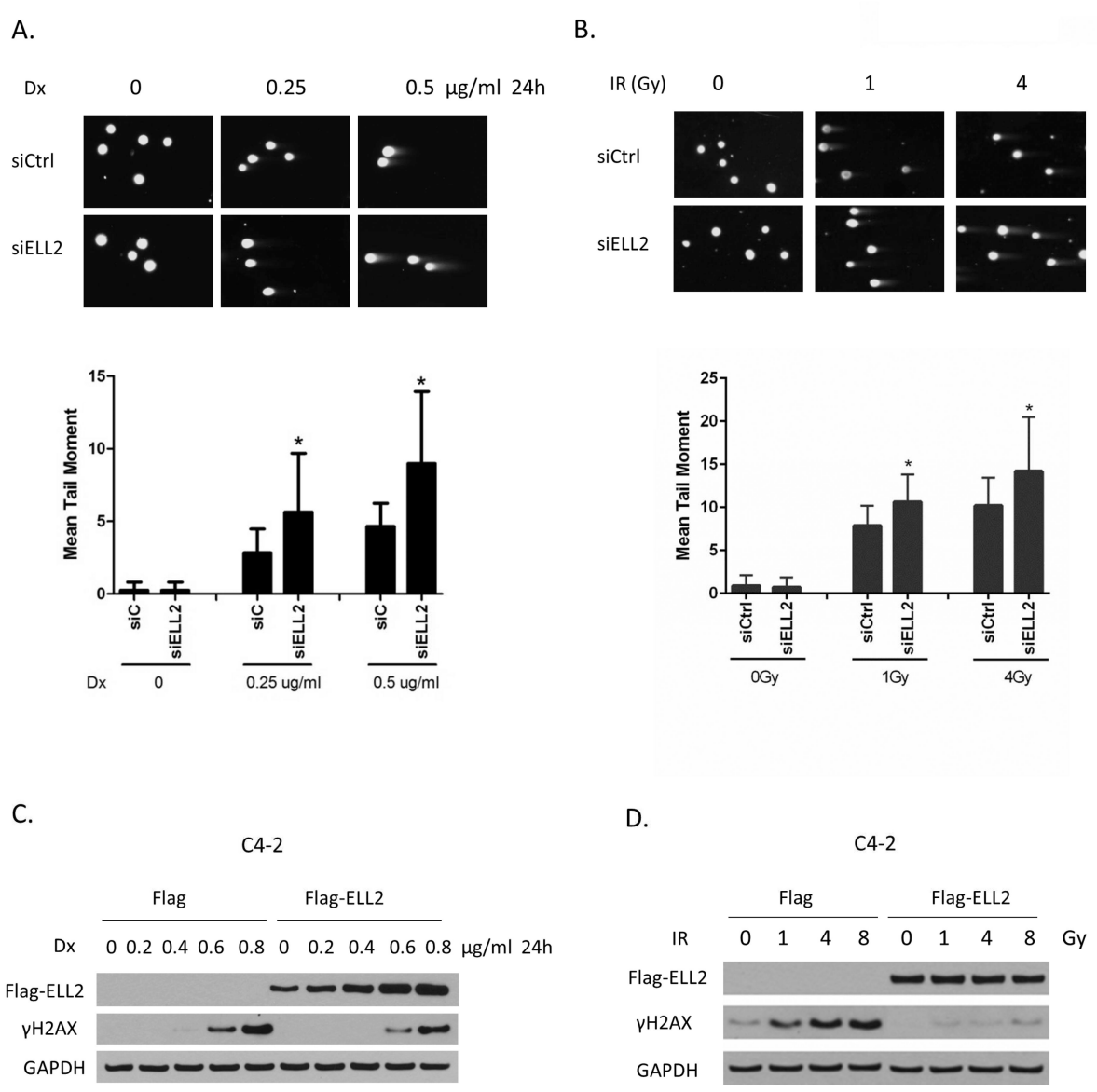

Figure 2. ELL2 protects prostate cancer cells from doxorubicin- or γ-irradiation-induced DNA damage

(A and B) Influence of ELL2 knockdown on single-cell neutral gel electrophoresis (COMET) assay of C4-2 cells. Cells were treated with siELL2 for 48 hours and then treated with doxorubicin (Dx, μg/ml) for 24 hours or γ-irradiation for 6 hours. The tail moments of 50 cells with or without irradiation were measured, and mean values with standard deviations are shown below. Error bars indicate SEM, *p<0.05. (C and D) Effect of overexpression of ELL2 on γH2AX induction by Dx or γ-irradiation in C4-2 cells. Cells were transfected with Flag-ELL2 or Flag expression vector for 48 hours and then treated with indicated dosages of Dx (0 – 0.8 μg/ml) for 24 hours or γ-irradiation (0 – 8 Gy) for 6 hours.

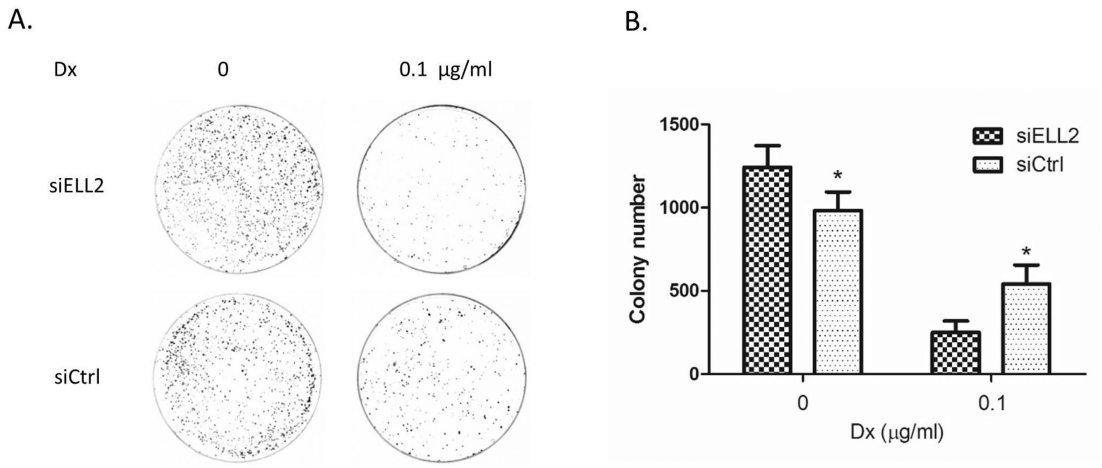

Figure 3. Knockdown of ELL2 reduces C4-2 cell colony formation upon doxorubicin treatment

(A) Colony formation assay. C4-2 cells were treated with siRNA for 48 hours, and then treated with doxorubicin (Dx, 0.2 μg/ml) for an additional 24 hours. Cells were plated in 10-cm plates at a density of 2000 cells/plate, and incubated for 14 days. (B) Colonies were counted by Image-Pro Plus software. Error bars indicate SEM. *$p<0.05$.

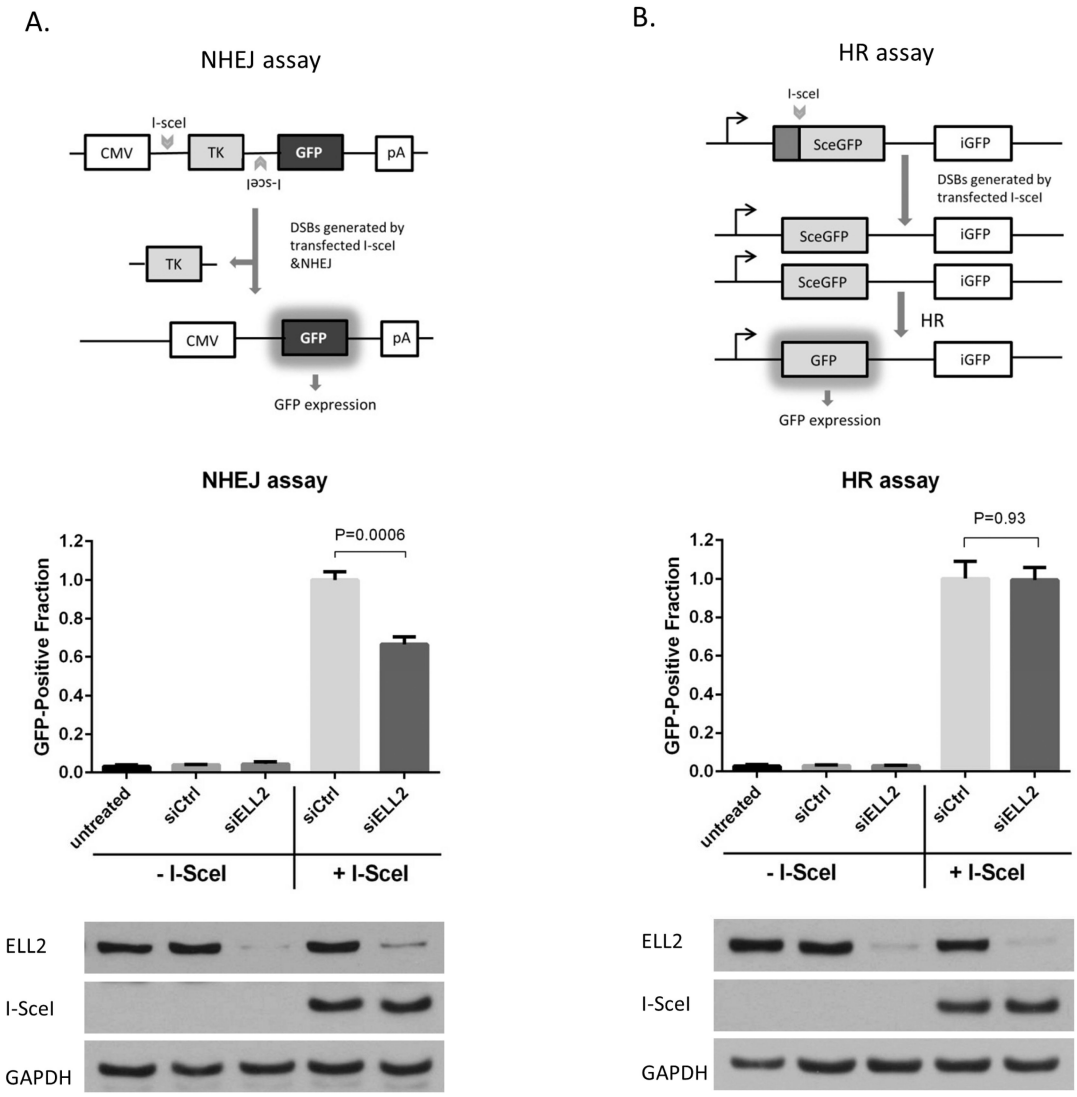

Figure 4. Knockdown of ELL2 impairs NHEJ, but not HR, of double-strand breaks (DSBs) in chromosomal DNA

(A) Assay for NHEJ of chromosomal DSBs in H1299 (dA3-1) cells. Top panel shows the design of the NHEJ assay. Transiently expressed I-SceI protein cleaves the I-SceI sites and produces DSBs with incompatible ends in the substrate. NHEJ repair of two broken DNA ends of chromosomal DNA results in EGFP expression. In the middle panel, GFP-positive fraction of cells treated with siELL2 or siCtrl indicates frequency of NHEJ repair of chromosomal DNA. In the lower panel, Western blot analysis confirmed knockdown of ELL2 and transfection of I-SceI expression. (B) Assay for HR frequency of chromosomal DNA containing a recombination substrate DR-GFP in HeLa cells. Top panel shows the design of the HR assay. In the middle panel, GFP-positive fraction of cells treated with siELL2 or siCtrl indicates frequency of HR repair of chromosomal DNA. In the lower panel, Western blot confirmed knockdown of ELL2 and transfection of I-SceI expression. Blots were reprobed with GAPDH antibody to provide protein loading control.

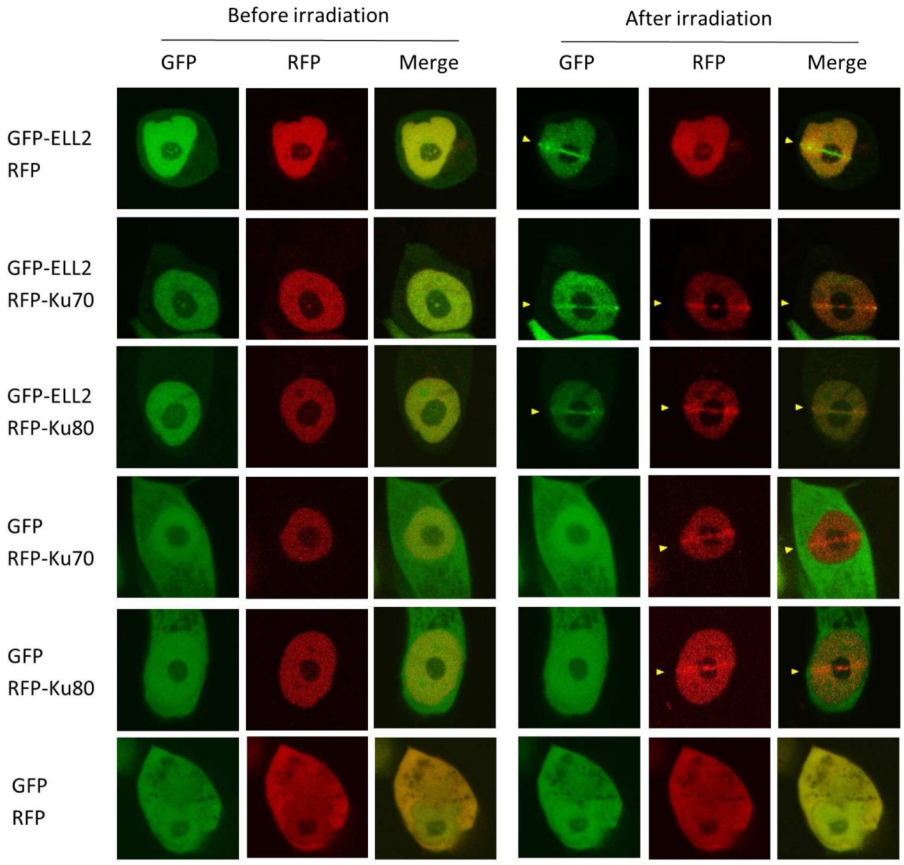

Figure 5. Response and co-accumulation of GFP-ELL2 and RFP-Ku70/80 proteins at DSBs sites after laser microirradiation

C4-2 cells were transiently transfected with GFP, GFP-tagged ELL2, RFP and/or RFP-tagged Ku70 or Ku80 expression vectors, and treated with laser microirradiation to induce DSBs 24 hours after transfection. Images were obtained immediately before or after irradiation. Accumulation of the transfected proteins was indicated by GFP (green) or RFP (red) fluorescence at laser-irradiated sites. Yellow arrowheads indicate direction of laser irradiation. Co-accumulation was visualized in merged images.

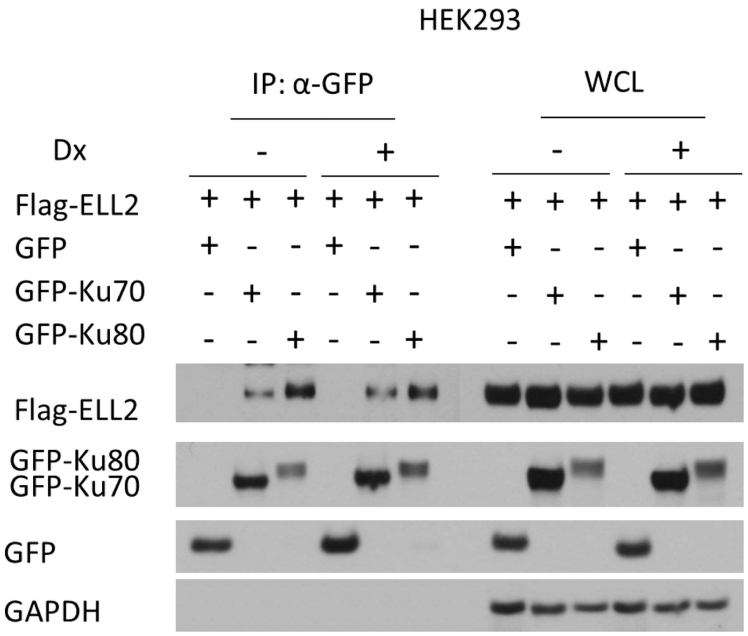

Figure 6. ELL2 binds to DNA repair proteins Ku70 and Ku80

Co-immunoprecipitation of transfected Flag-ELL2 with GFP-Ku70 and GFP-Ku80. HEK293 cells were transiently transfected with the mammalian expression vectors for Flag-ELL2 and GFP, GFP-Ku70, or GFP-Ku80. Whole cell lysates (WCL) were immunoprecipitated with immobilized anti-GFP protein G beads and immunoblotted with anti-Flag or anti-GFP.

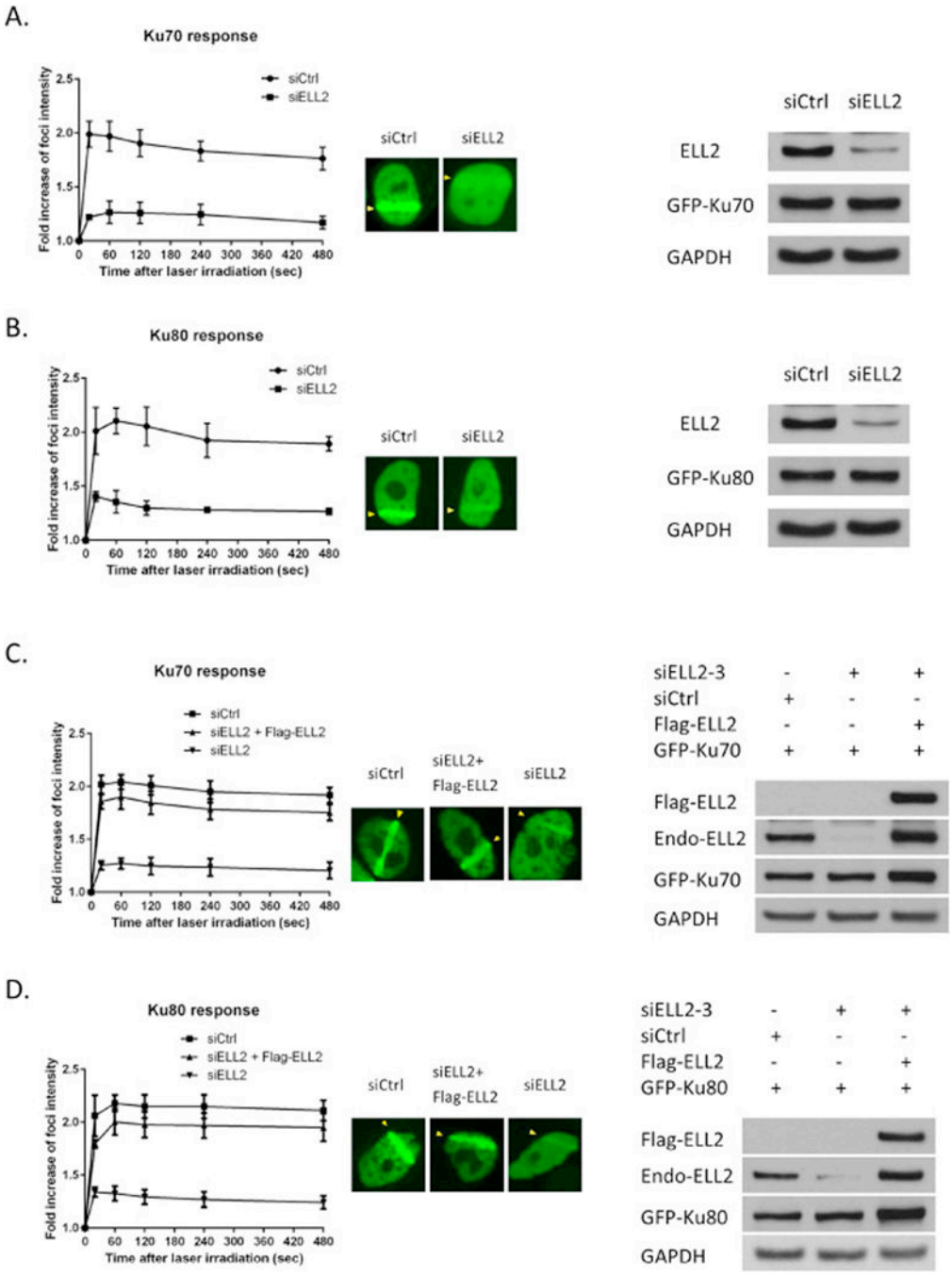

Figure 7. Knockdown of ELL2 impairs the recruitment of Ku70/80 at laser microirradiation-induced DSBs sites

(A) Foci intensity of GFP-Ku70 accumulation at sites of laser microirradiation in C4-2 cells treated with indicated siRNA(s) for 48 hours followed by transfection with GFP-Ku70. Mean foci intensity was measured every 20 seconds for 8 minutes and subtracted from background intensity (left panel). The middle panel shows the Ku-70 accumulation which was indicated by GFP fluorescence at laser-irradiated DNA damage sites. The right panel shows ELL2 knockdown and GFP-Ku70 expression. (B) Left panel shows the kinetics of GFP-Ku80 accumulation at laser-irradiated sites in C4-2 cells treated as described in (A).

The middle panel shows the Ku-80 accumulation and the right panel shows ELL2 knockdown and GFP-Ku80 expression. (C) C4-2 cells were treated with siELL2 for 48 hours. Cells were then transfected with GFP-Ku70 alone or combination of siELL2-resistant Flag-ELL2 expression vector for 24 hours. Left panel shows the kinetics of GFP-Ku70 accumulation at laser-irradiated sites. The middle panel shows the Ku-70 accumulation which was indicated by GFP fluorescence at laser-irradiated DNA damage sites. The right panel shows ELL2 knockdown and GFP-Ku70 and Flag-ELL2 expression. (D) Kinetics of GFP-Ku80 accumulation at laser-irradiated sites in C4-2 cells treated similarly to (C).

Table 1

siRNA sequences for ELL2

siELL2-1	AUUUACAAUCUGAGGAGGAUGUGAGAU
siELL2-2	CAGUAAUGUGCAAGGUGAAAUGCUU
siELL2-3	AGUAUGCUUCCCAUUGCUCUAAUCAAG